RESEARCH ARTICLE

Hair-Regrowing Potential of Minoxidil Nanocrystal Structure versus Rosemary's Hydroethanolic Extract on C57BL/6 Mice

Ali Moradi[1], Seyed Morteza Seifati[1*], Majid Darroudi[2,3*], Shiva Golmohammadzadehd[4,5], Mahmood Dehghani Ashkezari[1]

[1] Department of Biology, Medical Biotechnology Research Center, Ashkezar Branch, Islamic Azad University, Ashkezar, Yazd, Iran

[2] Nuclear Medicine Research Center, Mashhad University of Medical Sciences, Mashhad, Iran

[3] Department of Medical Biotechnology and Nanotechnology, Faculty of Medicine, Mashhad University of Medical Sciences, Mashhad, Iran

[4] Nanotechnology Research Center, Pharmaceutical Technology Institute, Mashhad University of Medical Sciences, Mashhad, Iran

[5] Department of Pharmaceutics, Faculty of Pharmacy, Mashhad University of Medical Sciences, Mashhad, Iran

ARTICLE INFO

Article History:
Received 13 Dec 2023
Accepted 21 Mar 2024
Published 01 Apr 2024

Keywords:
Minoxidil nanoparticles (MXD-NPs)
Human dermal fibroblast (HDF)
Cytotoxicity
C57BL/6 mice
Hair growth stimulating activity

ABSTRACT

This study aimed to enhance the effectiveness and water solubility of Minoxidil (MXD) by producing its nanocrystal structure, which improves its vasodilator properties and promotes hair growth. In the current study, the hair growth-stimulating activity of the MXD nanoparticles (MXD-NPs) was compared with the hydroethanolic rosemary (RSY) extract on the C57BL/6 mice. The MXD-NPs were produced through a bead mill and ultrasonic process and characterized using various techniques. The cytotoxicity of MXD-NPs was studied on human dermal fibroblasts, and their hair growth-stimulating activity was analyzed in C57BL/6 mice. The results showed that MXD-NPs significantly increased the hair growth rate in mice compared to commercial MXD and hydroethanolic rosemary extract as they were delivered safely and specifically to the target pilosebaceous follicles. The follicular uptake of MXD-NPs was also increased compared to commercial MXD, leading to improved pilosebaceous follicle re-growth and hair growth in treated mice. Therefore, MXD-NPs have the potential to be a safe and efficient iso-formulation structure for hair growth promotion.

How to cite this article
Moradi A., Seifati S.M., Darroudi M., Golmohammadzadehd Sh., Dehghani Ashkezari M. Hair-Regrowing Potential of Minoxidil Nanocrystal Structure versus Rosemary's Hydroethanolic Extract on C57BL/6 Mice. Nanomed Res J, 2024; 9(1): 90-102. DOI: 10.22034/nmrj.2024.01.010

INTRODUCTION

Alopecia, also known as hair loss, is a common skin disorder affecting approximately 50% of men and 40% of women [1-3]. The use of Minoxidil (MXD), a medication that promotes hair growth by increasing blood flow to hair follicles, is limited due to its potential side effects such as redness, itching, and inflammation. Additionally, the poor water solubility of MXD and the use of common toxic adjuvants like propylene glycol (PG) and ethanol can decrease its bioactivity and treatment efficiency [4-6]. The solvents used to dissolve MXD, such as PG/water/ethanol, can improve its bioaccessibility, but they may cause undesirable effects like burning, scalp dryness, dermatitis, irritation, and redness [7, 8].

Minoxidil nanocrystals represent a groundbreaking innovation in the field of hair growth treatments. These nanocrystals are tiny, solid particles of minoxidil, an FDA-approved medication for treating hair loss in both men and women. The development of minoxidil nanocrystals aims to

* Corresponding Author Email: *Seifati@gmail.com*
darroudim@mums.ac.ir

This work is licensed under the Creative Commons Attribution 4.0 International License.
To view a copy of this license, visit http://creativecommons.org/licenses/by/4.0/.

improve the drug's bioavailability, penetration, and efficacy, ultimately leading to better hair regrowth outcomes. By reducing the particle size of minoxidil, researchers have managed to enhance its solubility and stability, allowing for more effective delivery to the hair follicles.

In a study in 2019, Noriaki *et al*., synthesized minoxidil monocrystals. Minoxidil monocrystals have shown promising results in vitro and in vivo studies, demonstrating their potential to revolutionize hair growth treatments [9]. In comparison to traditional minoxidil solutions, nanocrystal-based formulations have exhibited enhanced percutaneous penetration, leading to a more significant reduction in hair loss and an improvement in hair thickness and density. Also, in a study in 2022, Yoshihide *et al.* prepared minoxidil monocrystals with a size of 139 nm [10]. Their results showed that minoxidil monocrystals significantly improved hair regrowth and overall hair health, providing a strong foundation for further development and clinical trials of this innovative treatment. As research progresses, minoxidil monocrystals may soon become a solution for people looking for effective and reliable hair growth treatments [11, 12].

MXD stimulates hair growth by opening potassium channels, inducing vascular endothelial growth factor (VEGF), and promoting prostaglandin synthesis in the dermal papilla [13-15]. Moreover, there are various types of herbal extracts have been administrated as hair-regrowing treatment compounds such as saw palmetto, peppermint, and rosemary [16-18].

Rosemary oil, derived from the herb rosemary, is one of the most popular and widely used herbal hair-regrowing compounds. This essential oil is rich in antioxidants and has anti-inflammatory properties that help to promote hair growth. Rosemary oil contains caffeic acid, which stimulates blood flow to the scalp, and carnosic acid, which prevents hair loss by inhibiting the production of DHT (dihydrotestosterone), a hormone that causes hair follicles to shrink [19].

There are two primary routes for skin penetration: the intercellular and trans-cellular routes, which utilize the lipids in the stratum corneum and corneocytes, respectively [20, 21]. The accumulation of drugs near hair follicles is crucial for follicular growth and differentiation [22]. To enhance the bioavailability and concentration of active compounds in the epidermal pilosebaceous follicles, various types of topical drug delivery systems (TDDS) have been developed [23-27]. The efficiency of MXD-loaded niosomes in topical skin treatments is greater than their unencapsulated forms in hairless mice, without skin penetration through hair [27]. Nanolipid carriers are a promising approach for targeting epidermal follicles due to their similarity to sebum structure, but they have limitations such as unspecific penetration from the skin epidermal layer and reduced transferred bioactive components [28]. Liposome-based delivery systems have a positively charged surface, which results in insufficient delivery into deeper epidermal layers due to the negatively charged upper skin epidermal layer and enhanced accumulation and localization of bioactive components at undesired epidermal regions [28-30]. Nanoparticles with a size of 100 nm have been found to have significantly improved penetration into hair follicles [31]. These nanoparticles are suitable for targeted localization and controlled release of bioactive compounds in dermal therapies, as supported by studies carried out by researchers [32, 33]. The current study aims to discover a novel technique for incorporating effective localization and targeted delivery of bioactive substances into drug delivery systems that have not been explored before. In this regard, MXD-NPs have been produced using bead mill and ultrasonic methods. The structural and optical properties of these nanoparticles were investigated using various techniques, including dynamic light scattering (DLS)/Zeta, UV-Vis, Fourier transform infrared (FTIR), X-ray diffraction (XRD), Transmission electron microscopy (TEM), and Field emission scanning electron microscopy (FESEM)/Particle size analyzer (PSA)/Energy-dispersive X-ray (EDX). Moreover, the cytotoxicity of synthesized MXD-NPs was evaluated on human dermal fibroblast (HDF) cell lines, and their hair-growing activity was evaluated by observing hair growth on treated c57BL/6 mice.

MATERIAL AND METHODS

Materials

The substances hydroethanilic rosemary extract, methylcellulose (MC), and minoxidil were supplied by Merck company based in Germany. The phosphate buffer saline (PBS), Dulbecco's modified eagle medium (DMEM), and dimethyl sulfoxide (DMSO) were obtained from Gibco Company. The 3-(4, 5-dimethylthiazol-2)-2, 5 diphenyl

tetrazolium bromide (MTT) was purchased from Merck company located in Germany. Additionally, a specific human dermal fibroblast cell line (HDF, code F-1049024) was provided by the Pasture Institute of Iran.

Production of Minoxidil nanoparticles

To prepare MXD-NPs, 0.50 g of MXD powder and 1.0 g of MC powder were mixed and ground in an agate mortar for 2 hours at a temperature of 5 °C. This mixture was added in 100 mL of distilled water, and then zirconia beads with a diameter of 0.10 mm were added to the dispersed solution. The mixture was homogenized by subjecting it to ultrasonic waves for 4 min at a temperature of 5 °C, alternately repeated 25 times. The resulting MXD-NPs were stored in the dark and at low temperatures.

Characterization of MXD-NPs

The size and stability of the MXD-NPs were measured using DLS and Zeta potential analysis, respectively. The stability test was performed twice, both immediately after preparation and after 3 months of storage in dark conditions at room temperature. To study the size, shape, and chemical composition of MXD-NPs, FESEM and EDX were employed. The crystal structure of MXD-NPs was analyzed using the XRD technique. Also, the morphology of MXD-NPs was observed through TEM images. The UV-Visible spectrum was utilized to examine the stability of MXD-NPs. The FTIR technique was employed to analyze the functional groups and molecular bonds present in MXD-NPs.

MXD-NPs' Cytotoxicity

The cytotoxicity of MXD-NPs was evaluated on human dermal fibroblast (HDF) cells. Specifically, 2.5×10^3 cells were seeded into 96-well plates and cultured in DMEM medium supplemented with 15% FBS, Gluta MAX (1%), antibiotic (streptomycin 100 µg/mL-penicillin 100 µg/mL), and amphotericin B 250 µg/mL. Different concentrations of MXD-NPs (1.5, 3, 6, 12, 25, 50, and 100 µg/mL) were added to each well and incubated for 24 h. Afterward, fresh MTT solution (5 mg/mL in PBS) was added to the treated cells and incubated for an additional 3 h. To dissolve the insoluble formazan produced by the cells, DMSO (100 µL) was added to each well and incubated for 15 min while shaking. Then absorbance was measured at a wavelength of 570 nm using an ELISA reader (Epoch, Model 680, Japan). The relative cell viability (%) was calculated using **Eq. 1**.

$$Viability\ (\%) = \left[\frac{\text{Absorbance of treated cells} - \text{Absorbance of blank}}{\text{Absorbance of control cells} - \text{Absorbance of blank}}\right] \times 100 \quad (1)$$

where "control cells" refer to the untreated cells, "treated cells" refer to the cells exposed to MXD-NPs at different concentrations, and "blank" refers to the wells without any cells or treatments.

Preparation and treatment of Hairless mice model (HMM)

In this study, 36 male C57BL/6 mice, each weighing 18-20 g and six weeks old, were obtained from the Pastor Institute of Iran. The mice were housed in standard conditions with a 12-hour light/dark cycle, a temperature of 22 ± 1°C, and a humidity level of 60 ± 10%. The mice acclimated to their surroundings for a week before treatment and were then randomly assigned to one of six different groups receiving various treatments. The mice' necks and backs were shaved (2 × 2 cm) and kept in separate cages. Following the topical application of MXD-NPs, the mice received a daily massage for two minutes in both hair growth directions based on their assigned group. Treatment was administered for 28 consecutive days. The first group did not receive any treatment (negative control), while the second and third treated groups received MXD-NPs (0.5%) and 2% commercial MXD (positive control), respectively. The fourth group received only massage therapy. The fifth group was treated with a combined mixture containing MXD-NPs: Rosemary extract (9:1 V/V), and the sixth group received rosemary extract.

Measuring the MXD-NPs hair re-growth stimulating activity

The hair regrowth and skin color changes in the shaved area of the HMM (human-mouse hybrid) were documented using a high-resolution camera, Nikon D5000, at various time points (0, 7, 14, 21, and 28 days). The images were analyzed using image-J software® and were assigned scores based on the following scale: 0 = pink color, that indicating no pigmentation, 1 = up to 20% darkening, 2= 20-50%, 3 = 50–70%, 4 = 70–90%, 5 = 90–100%, and 6 = 20–50% hair-regrowth [34, 35].

Measuring the HMM histopathology

During a 28-day treatment period,

(cc) BY

experimental mice underwent a therapeutic regimen. Following this intervention, the mice were humanely euthanized, and 2×2 cm^2 biopsies were obtained and preserved in formalin. The specimens were subsequently forwarded to the pathology laboratory at Ghaem Hospital in Mashhad for paraffin embedding. The follicle count was determined at three distinct cross sections for each skin sample using a×40 magnification. The slides were then analyzed using Image-J software* (×40 magnification) to estimate the size and pigmentation of the follicles.

Statistics

To assess the normality of the data, the Shapiro-Wilk test was employed. For normally distributed data, an analysis of variance (ANOVA) was utilized. In binary comparisons, the Tukey test was implemented. For non-normally distributed data, the Kruskal-Wallis test was applied. Lastly, the Don-Bonferroni test was carried out to examine the statistical significance of pairs.

RESULT AND DISCUSSION

Characterization of MXD-NPs

According to FESEM imaging and size distribution analysis (PSA), the morphology of MXD-NPs was found to be spherical with a mean size of 49 nm (**Fig. 1(a)** and **Fig. 1(c)**). This result was confirmed by TEM/PSA (**Fig. 1(b)** and **Fig. 1(d)**) and XRD techniques (**Fig. 2(a)**). The XRD diagram of bulk MXD crystals (**Fig. 2a**, right corner) exhibited sharp peaks at 2θ of 12.52°, 15.64°, 16.44°, 19.62°, 21.62°, 22.62°, and 23.12°, which also were observed in the diffractogram of MXD-NPs. However, there were some differences

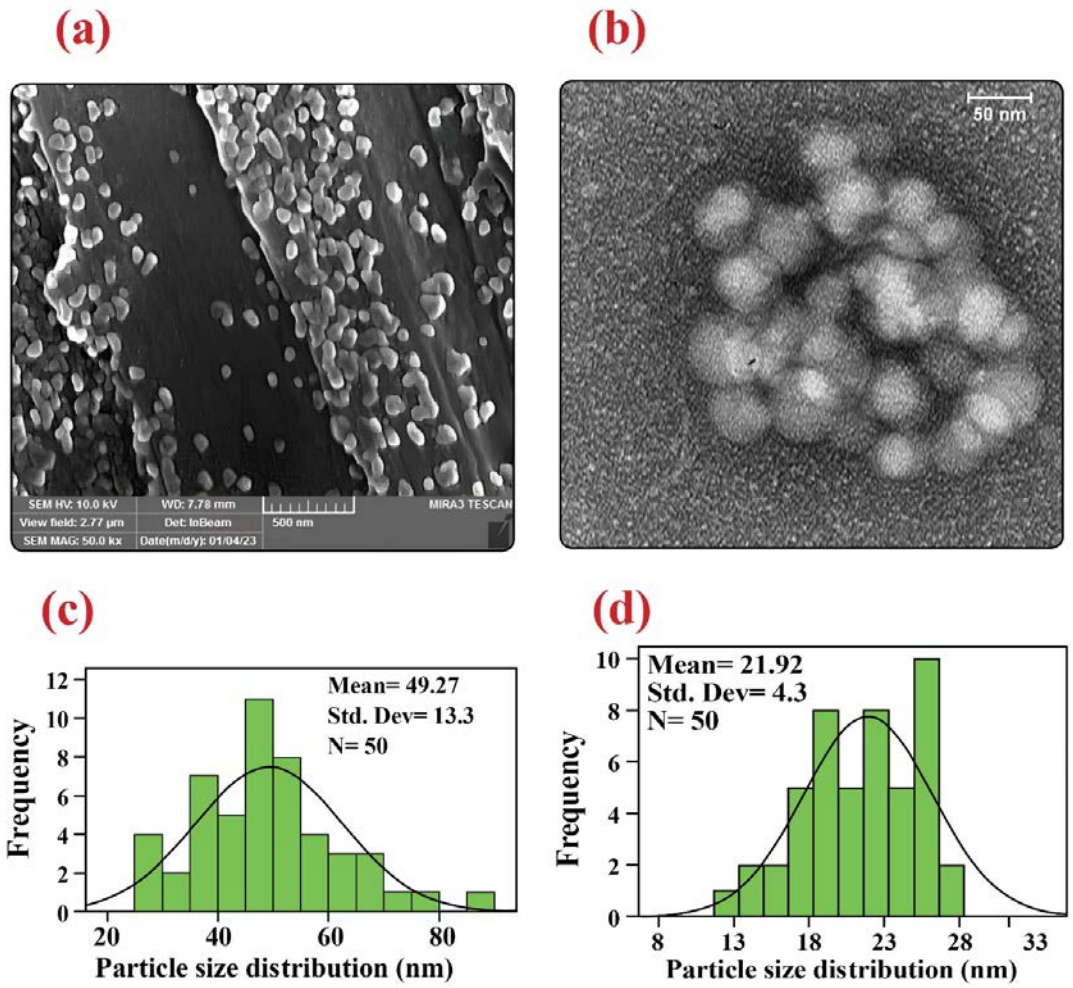

Fig. 1. FESEM image (a), TEM image (b), PSA histogram of MXD-NPs FESEM (c) and TEM (d).

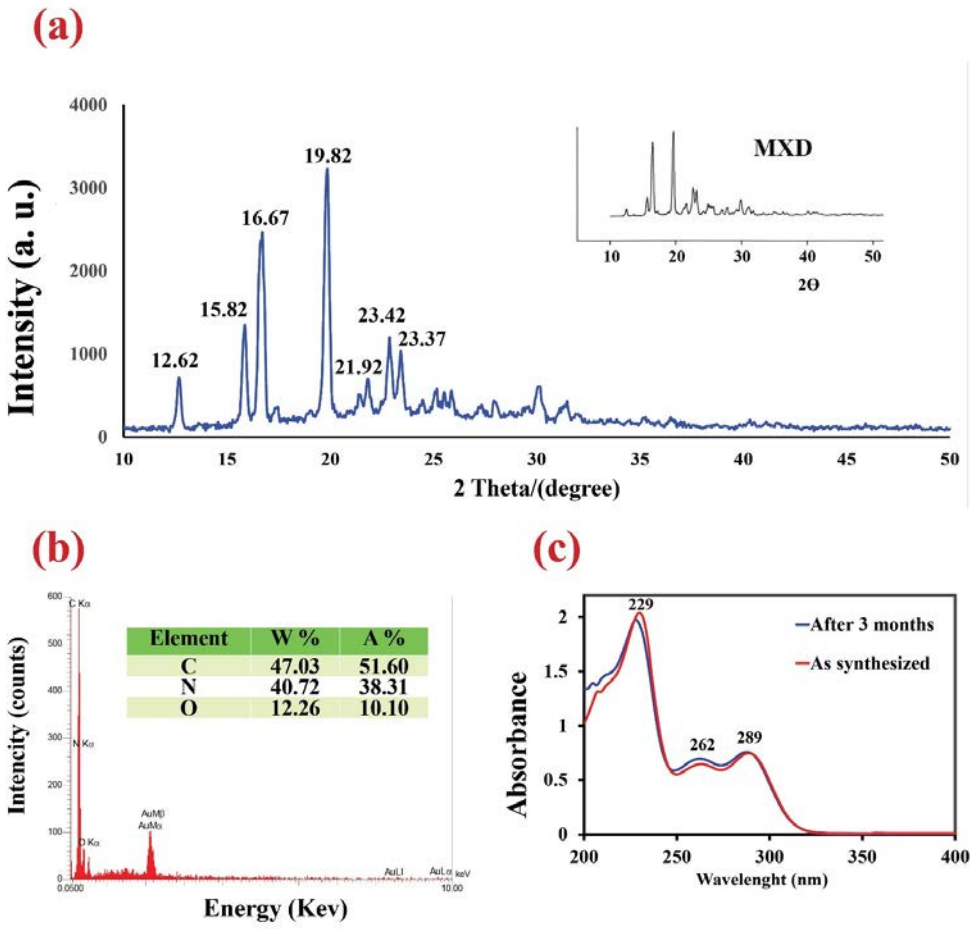

Fig. 2. The XRD pattern (a), EDX (b), and UV-Vis spectra of synthesized MXD-NPs (c).

in peak position and intensity, indicating a novel and improved arranged crystalline structure due to irradiation-mediated tensile stress (**Fig. 2(a)**) [36, 37]. The FTIR analysis further verified the crystalline alteration in MXD-NPs by showing lower intensities at specific wavenumbers compared to the commercial bulk MXD FTIR spectrum (**Table. 1, Fig. 3**). The peaks at 3423.64 cm^{-1} and 1645.28 cm^{-1} corresponded to N-H stretching and bending bonds of primary amine, respectively, while the peak at 1462.16 cm^{-1} represented the C=C stretching bonds of the aromatic cycle. Also, C-N stretching bonds appeared at 1233.60 cm^{-1} [38].

The size of MXD-NPs was measured to be approximately 62 nm using DLS analysis (**Fig. 4(a)**). The stability of MXD-NPs was confirmed through zeta potential analysis, which revealed a negative value of -46 mV (**Fig. 4(b)**). The presence of structural oxygen with a negative charge in the O-N bond of MXD is attributed to the new crystal form, which facilitates better permeation into the skin and enhanced stability in water solutions [29]. The UV-Vis technique was utilized to confirm the synthesis and stability of MXD-NPs over a three-month storage period at 25 °C in dark conditions. The maximum wavelengths of MXD were observed at 229, 262, and 282 nm (**Fig. 2(c)**), and the gradual decrease in absorption intensity over three months indicates the chemical stability of MXD-NPs.

Cytotoxicity of MXD-NPs

The safety of MXD-NPs was assessed on normal human dermal fibroblast (HDF) cells. The results revealed that after 24 h of incubation, there was no significant cytotoxicity observed at various concentrations of MXD-NPs (1.5, 3, 6, 12, 25, 50, and 100 µg/mL) (**Fig. 5**). This is while the cells exposed to hydroethanolic rosemary extract

(cc) BY

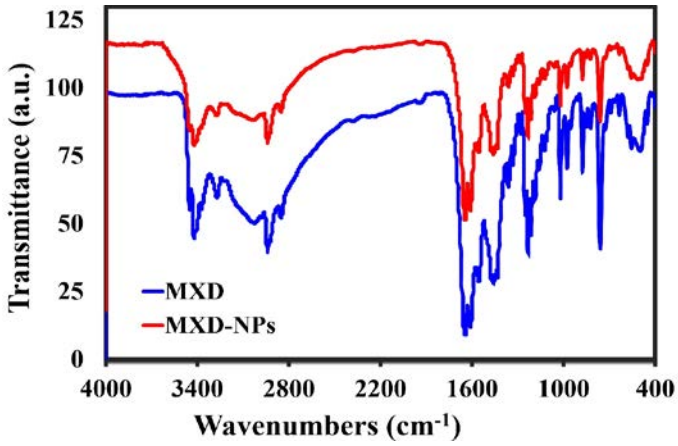

Fig. 3. FTIR spectra of bulk MXD and synthesized MXD-NPs.

Table. 1. The sharp peaks of pure MXD and synthesized MXD-NPs in FTIR spectra.

Sample	Vibrations (cm^{-1})					
Bonds	**N-H Stretching**	**N-H Bending**	**C=C Aromatic stretching**	**C-N Stretching**	**C-N Stretching**	**N-H Stretching**
MXD-NPs	3423.07	1645.95	1462.05	1233.55	1210.00	758.58
Pure MXD	3423.64	1645.28	1462.16	1233.60	1210.59	757.70

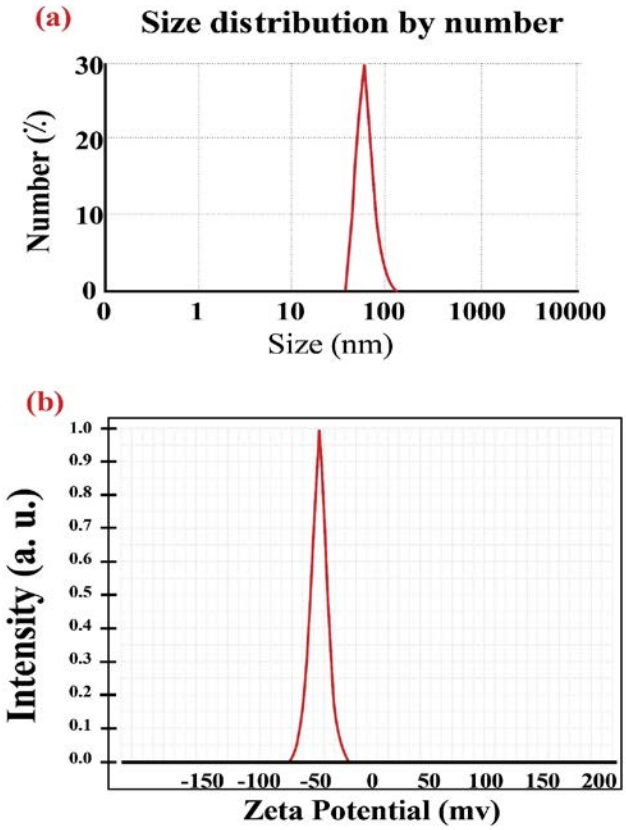

Fig. 4. DLS (a) and Zeta potential of MXD-NPs (b).

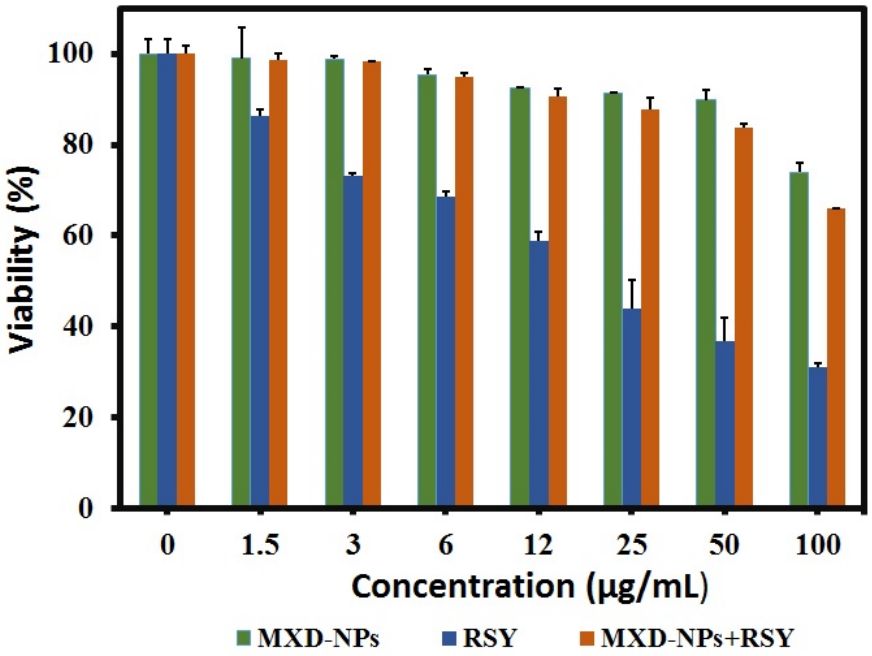

Fig. 5. Cytotoxic of MXD-NPs on HDF cell lines.

meaningfully reduced cell survival. Based on the findings, it can be due to the dominant toxicity of ethanol. The results showed that MXD-NPs are non-toxic on normal fibroblasts at concentrations less than or equal to 50 µg/mL. This suggests that doses of MXD-NPs below 50 µg/mL are not toxic to normal HDF skin cells.

MXD-NPs' impact on hair-cycled stimulation

To assess the impact of MXD-NPs on hair regrowth in C57BL/6 mice, their dorsal hair was shaved the day before treatment began. The hair regrowth was compared to that of untreated and MXD (2%) treated mice, which is currently considered the gold standard. The pink color in the images represents the shaved skin during the telogen phase, and the dark (gray) region represents the initiation of anagen [39-41]. After 7 days of treatment, dark regions appeared on the dorsal skin due to follicles entering the anagen phase (**Fig. 6(a)**). Mice treated with MXD-NPs had wider dark regions compared to the control group. After 14 days, mice treated with MXD-NPs had a greater hair regrowth area (80%) on their dorsal skin compared to those treated with standard MXD (70%). Interestingly, after 28 days of treatment, mice in the control group had fully regrown hair, while mice treated with MXD-NPs also had fully regrown hair on their dorsal skin. This suggests that MXD-NPs have the potential to replace current commercial MXD for improving hair follicle regrowth [42].

After a 21-day treatment period, the average regrowth of hair in the untreated mice was approximately 5.5 mm, as demonstrated in (**Fig. 6(b)**). Mice that received MXD at a concentration of 2% (w/v) had a hair regrowth value of 7.2 mm. In contrast, mice exposed to MXD-NPs at a concentration of 0.5% (w/v) exhibited a longer hair regrowth value of 7.9 mm. Even though the MXD formulation used in this study contained four times the concentration of bioactive ingredients compared to the synthesized MXD-NPs, the efficiency, and safety of the MXD-NPs were greater than those of the commercial formulation. The improved safety of MXD-NPs was confirmed by observing that there was no formation of non-keratinized skin in the local area following topical application of MXD-NPs, which supports this claim **(Fig. 6(b))** [33].

Pathology

The study found that the size and number of hair follicles in mice treated with MXD-NPs were significantly greater compared to those in the control groups (**Fig. 7(a)**). Additionally, the morphology of the epidermis was similar among all treatment groups (**Fig. 7(a)**). For further analysis,

(cc) BY

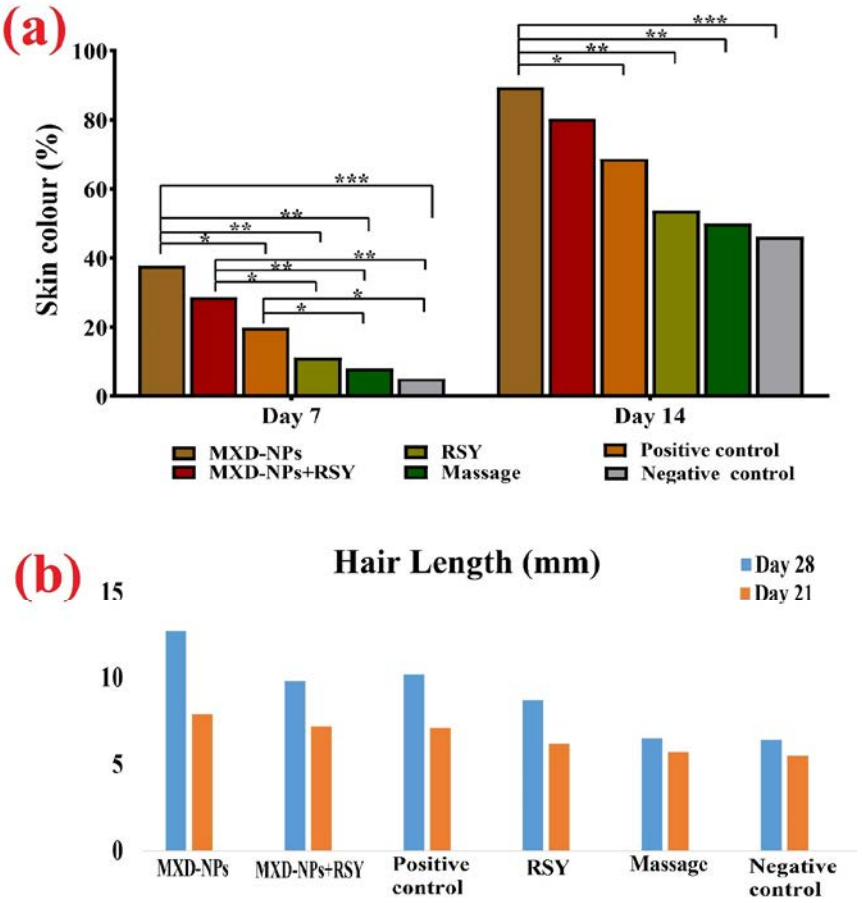

Fig. 6. The anagen phase induction (a) and hair length pattern (b) of the C57BL/6 mice following 28-day MXD-NPs treatment (N=6); Data are expressed as mean ± SD. ***P <0.001.

the authors presented pathological images of hair follicles showing an increase in the number of anagenic follicles and an increase in the follicular area. These images revealed anagenic follicles that were detectable following staining and confirmed the anagenic phase at the follicle cycle. The mean anagenic hair follicle counts for longitudinal sections of mice treated with MXD-NPs, MXD (2%), Rosemary extract, and MXD-NPs-Rosemary were 25.5±2.90, 19.81±2.82, 15.27±3.9 and 21.29±3.16, respectively (**Fig. 7(b)**). The results suggest that MXD-NPs have the potential to stimulate hair development, as described in previous studies [43].

Hair growth algorithm in treated mice

To investigate the impact of MXD-NPs on hair growth, mice were randomly divided into 6 groups and topically treated with MXD, MXD-NPs, RSY, MXD-NPs+RSY, and massage-therapy every day for 4 weeks (28 days) compared with the negative control group. The areas where hair had grown and turned dark were observed. The mice that received MXD-NPs showed a significant increase in the darkened skin area compared to the group treated with 2% MXD. The back skin hair of the treated mice was found to be in the mature anagen phase. After 7, 14, 21, and 28 days of treatment, the hair growth score was evaluated. The mice that received MXD-NPs had significantly enhanced hair growth compared to the untreated group after 7 and 14 days of treatment. This is while the mice exposed to RSY and MXD-NPs+RSY did not exhibit significant hair regrowth improvement. The findings suggest that treatment with MXD-NPs may promote hair growth by accelerating the transition from early telogen to anagen in C57BL/6 mice compared to 2% MXD and RSY treatment [43].

In recent studies, various types of hair regrowth inducers, including MXD, are widely consumed globally [44-46]. The nonpolar structure of MXD is

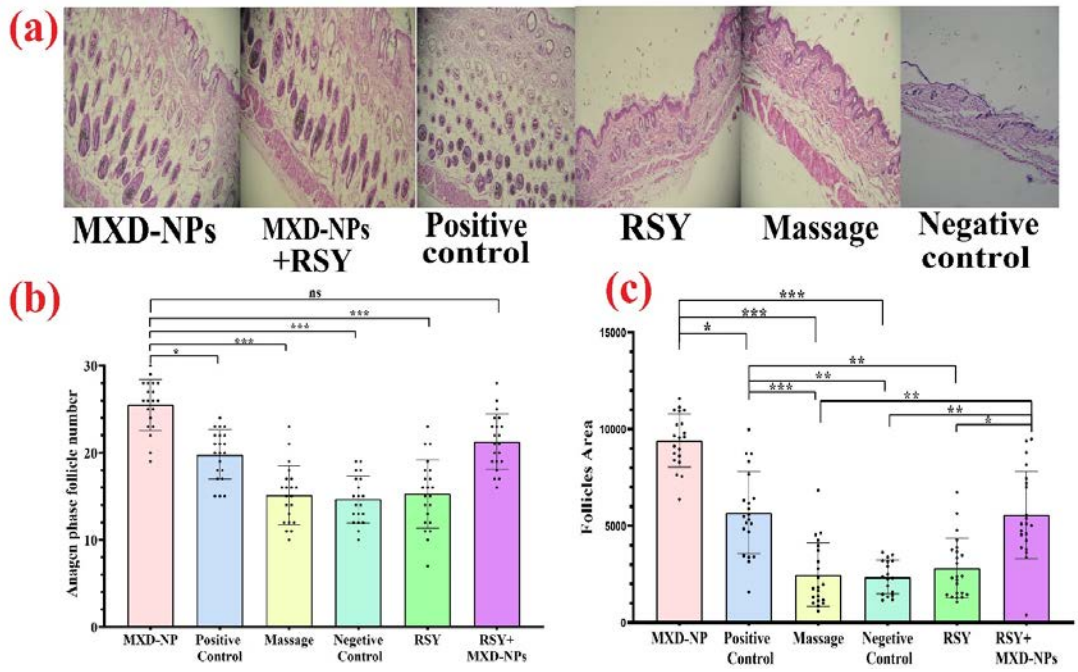

Fig. 7. Skin photomicrographs of the hair follicle growth in male C57BL/6 mice receiving MXD-NPs, MXD, RSY, MXD-NPs+RSY, Massage, and Negative control for 28 days. Histology results of the treated mice (original magnification) (a), represent the number of anagenic hair follicle counts and follicle area in histopathology sections, respectively (b) and (c). (N = 6; *P < 0.05, **P < 0.01, and ***P < 0.001.

Fig. 8. Hair growth scores scoring index (0 = no growth (pink color), 1 = up to 20% darkening, 2= 20-50%, 3 = 50–70%, 4 = 70–90%, 5 = 90–100%, and 6 = 20–50% hair-regrowth) (a) and Photometric evaluation of C57BL/6 mouse post-shaved hair growth after 0, 7, 14, 21, and 28 days (N= 6/mouse) (b).

commonly solved using nonpolar solvents, which have potentially toxic impacts. To address this issue, the current study substituted nonpolar solvents with polar types by crystalizing the structure of MXD. Additionally, the follicular uptake of crystal MXD was compared with its commercial form. The results indicate a significant improvement in hair regrowth in mice treated with crystal MXD compared to massage therapy and commercial MXD.

MXD was initially introduced as a hypertension treatment compound in the 1970s [47, 48]. It is a peripheral vasodilator that reduces peripheral vascular resistance and decreases blood pressure. MXD is also known for its hair regrowth properties [49]. However, hypertrichosis, a common side effect of MXD consumption, has been reported [50-52]. MXD enhances blood circulation near hair follicles, prolongs the anagen phase, and minimizes the impact of testosterone on hair follicles by converting it into another androgen [45, 49, 53-55]. It can also open potassium channels, release nitric oxide, and enhance blood flow around hair follicles, which are considered anagen phase prolonger factors [47, 56, 57]. Additionally, several adenosine receptors in dermal papilla cells (DPCs) and adenosine ligands act as MXD-mediated vascular endothelial growth factor (VEGF) production and stimulate hair growth [58].

The commercially available topical formulations of MXD contain ethanol and propylene glycol and have been associated with various types of skin damage such as rash, pruritus, dandruff, and allergic dermatitis [57, 59, 60]. To address this issue, several nano-based formulations containing MXD have been developed as topical drug delivery systems. These include penetration-enhancing vesicles (140-195 nm) [61, 62], foams (260-280 nm) [63, 64], lipid nanocarriers (177-194 nm) [65-67], microneedles (4150-4500 nm) [68-72], niosomes (214-252 nm) [27], and microbubbles [68]. The crystallized form of MXD has also been developed to improve its uptake. The results indicate enhanced hair growth rates in mice treated with MXD-NPs compared to commercial MXD and other non-pharmacological treatment strategies such as massage therapy. Additionally, the MXD-NPs did not exhibit significant cytotoxic impacts on HDF normal cell lines.

CONCLUSIONS

The use of nanostructures of minoxidil has been studied in previous research, with promising results. The MXD-NPs showed a significant increase in hair growth compared to the commercial formulation. This is likely due to the enhanced penetration and retention of the drug in the hair follicles, as well as the reduced irritation and toxicity associated with nanoparticle delivery. Therefore, the development of MXD-NPs represents a significant advancement in hair regrowth therapy. In other words, the MXD-NPs have a unique capability to be absorbed through the skin, which could increase their uptake and decrease unwanted side effects, offering a safer and more effective alternative to traditional minoxidil formulations. The smaller size of the MXD-NPs not only improves their chemical stability but also enhances their ability to be absorbed through the skin and promote hair follicle growth. However, further research is necessary to understand the specific mechanisms by which MXD-NPs affect hair follicle metabolism and proliferation.

ACKNOWLEDGMENTS

The authors are grateful to the Islamic Azad University of Ashkezar and Mashhad University of Medical Sciences for the technical support of this work based on the Ph. D thesis of Mr. A. Moradi

AUTHORS' CONTRIBUTIONS

Ali Moradi: Writing original draft, Data acquisition, Analysis, and interpretation. Seyed Morteza Seifati: Supervision, Data curation, Writing - review & editing. Majid Darroudi: Supervision, Project administration, Writing - review & editing, Funding, and resources acquisition. Shiva Golmohammadzadeh: Data curation, Writing - review & editing. Mahmood Dehghani Ashkezari: Data curation, Analysis, Writing - review & editing.

FUNDING

Not applicable

CONSENT TO PARTICIPATE

Not applicable

AVAILABILITY OF DATA AND MATERIAL

Not applicable

CONFLICTS OF INTEREST/COMPETING INTERESTS

The authors have declared no conflict of interest.

ETHICS APPROVAL AND CONSENT TO PARTICIPATE

All experiments were approved by the Research

Ethics Committee of the Islamic Azad University of Yazd (Etic code: IR.IAU.YAZD.REC.1400.047).

REFERENCE

1. Falto-Aizpurua L, Choudhary S, Tosti A. Emerging treatments in alopecia. Expert Opin Emerg Drugs, 2014;19 (4):545-556.
2. Rogers NE, Avram MR. Medical treatments for male and female pattern hair loss. Journal of the American Academy of Dermatology, 2008;59 (4):547-566.
3. Higgins CA, Christiano AM. Regenerative medicine and hair loss: how hair follicle culture has advanced our understanding of treatment options for androgenetic alopecia. Regenerative medicine, 2014;9 (1):101-111.
4. Al-Attar TS, Kawther K, Al-Neami MA, AbdulSahib WS. Colored asphalt and street print are decorating paving in public spaces. MATEC Web of Conferences, 2018;162:05027.
5. Mirzaeei S, Pirhayati FH, Mohammadi G, Rahimpour E, Martinez F, Jouyban A. Solubility of minoxidil in binary mixture of ethanol+ water at various temperatures. Physics and Chemistry of Liquids, 2019;57 (6):788-799.
6. Aljuffali IA, Sung CT, Shen F-M, Huang C-T, Fang J-Y. Squarticles as a lipid nanocarrier for delivering diphencyprone and minoxidil to hair follicles and human dermal papilla cells. The AAPS journal, 2014;16:140-150.
7. Nagai N, Iwai Y, Sakamoto A, Otake H, Oaku Y, Abe A, Nagahama T. Drug delivery system based on minoxidil nanoparticles promotes hair growth in C57BL/6 mice. International Journal of Nanomedicine, 2019;14:7921.
8. Desai C. Meyler's side effects of drugs: The international encyclopedia of adverse drug reactions and interactions. Indian Journal of Pharmacology, 2016;48 (2):224.
9. Nagai N, Iwai Y, Sakamoto A, Otake H, Oaku Y, Abe A, Nagahama T. Drug delivery system based on minoxidil nanoparticles promotes hair growth in C57BL/6 mice. International Journal of Nanomedicine, 2019:7921-7931.
10. Oaku Y, Abe A, Sasano Y, Sasaki F, Kubota C, Yamamoto N, Nagahama T, Nagai N. Minoxidil nanoparticles targeting hair follicles enhance hair growth in C57BL/6 mice. Pharmaceutics, 2022;14 (5):947.
11. Dubey SK, Dey A, Singhvi G, Pandey MM, Singh V, Kesharwani P. Emerging trends of nanotechnology in advanced cosmetics. Colloids and surfaces B: Biointerfaces, 2022;214:112440.
12. Vañó-Galván S, Camacho F. New treatments for hair loss. Actas Dermo-Sifiliográficas (English Edition), 2017;108 (3):221-228.
13. Rathnayake D, Sinclair R. Male androgenetic alopecia. Expert Opinion on Pharmacotherapy, 2010;11 (8):1295-1304.
14. Bassino E, Gasparri F, Munaron L. Protective role of nutritional plants containing flavonoids in hair follicle disruption: A review. International Journal of Molecular Sciences, 2020;21 (2):523.
15. Rossi A, Cantisani C, Melis L, Iorio A, Scali E, Calvieri S. Minoxidil use in dermatology, side effects and recent patents. Recent patents on inflammation & allergy drug discovery, 2012;6 (2):130-136.
16. Evron E, Juhasz M, Babadjouni A, Mesinkovska NA. Natural hair supplement: friend or foe? Saw palmetto, a systematic review in alopecia. Skin appendage disorders, 2020;6 (6):329-337.
17. Oh JY, Park MA, Kim YC. Peppermint oil promotes hair growth without toxic signs. Toxicological research, 2014;30:297-304.
18. Panahi Y, Taghizadeh M, Marzony ET, Sahebkar A. Rosemary oil vs minoxidil 2% for the treatment of androgenetic alopecia: a randomized comparative trial. Skinmed, 2015;13 (1):15-21.
19. Micić D, Đurović S, Riabov P, Tomić A, Šovljanski O, Filip S, Tosti T, Dojčinović B, Božović R, Jovanović D. Rosemary essential oils as a promising source of bioactive compounds: Chemical composition, thermal properties, biological activity, and gastronomical perspectives. Foods, 2021;10 (11):2734.
20. Beloqui A, Solinís MÁ, Rodríguez-Gascón A, Almeida AJ, Préat V. Nanostructured lipid carriers: Promising drug delivery systems for future clinics. Nanomedicine: Nanotechnology, Biology and Medicine, 2016;12 (1):143-161.
21. Ruela ALM, Perissinato AG, Lino MEdS, Mudrik PS, Pereira GR. Evaluation of skin absorption of drugs from topical and transdermal formulations. Brazilian Journal of Pharmaceutical Sciences, 2016;52:527-544.
22. Desai PR, Shah PP, Hayden P, Singh M. Investigation of follicular and non-follicular pathways for polyarginine and oleic acid-modified nanoparticles. Pharmaceutical research, 2013;30 (4):1037-1049.
23. Singh Malik D, Mital N, Kaur G. Topical drug delivery systems: a patent review. Expert opinion on therapeutic patents, 2016;26 (2):213-228.
24. Sinico C, Fadda AM. Vesicular carriers for dermal drug delivery. Expert opinion on drug delivery, 2009;6 (8):813-825.
25. Cosco D, Celia C, Cilurzo F, Trapasso E, Paolino D. Colloidal carriers for the enhanced delivery through the skin. Expert opinion on drug delivery, 2008;5 (7):737-755.
26. Cilurzo F, Chiara Cristiano M, Di Marzio L, Cosco D, Carafa M, Anna Ventura C, Fresta M, Paolino D. Influence of the supramolecular micro-assembly of multiple emulsions on their biopharmaceutical features and in vivo therapeutic response. Current Drug Targets, 2015;16 (14):1612-1622.
27. Balakrishnan P, Shanmugam S, Lee WS, Lee WM, Kim JO, Oh DH, Kim D-D, Kim JS, Yoo BK, Choi H-G. Formulation and in vitro assessment of minoxidil niosomes for enhanced skin delivery. International journal of pharmaceutics, 2009;377 (1-2):1-8.
28. Lauterbach A, Müller-Goymann CC. Applications and limitations of lipid nanoparticles in dermal and transdermal drug delivery via the follicular route. European Journal of Pharmaceutics and Biopharmaceutics, 2015;97:152-163.
29. Jung S, Otberg N, Thiede G, Richter H, Sterry W, Panzner S, Lademann J. Innovative liposomes as a transfollicular drug delivery system: penetration into porcine hair follicles. Journal of Investigative Dermatology, 2006;126 (8):1728-1732.
30. Jain B, Singh B, Katare OP, Vyas SP. Development and characterization of the minoxidil-loaded liposomal system for delivery to pilosebaceous units. Journal of Liposome Research, 2010;20 (2):105-114.
31. Toll R, Jacobi U, Richter H, Lademann J, Schaefer H, Blume-Peytavi U. Penetration profile of microspheres in follicular targeting of terminal hair follicles. Journal of Investigative Dermatology, 2004;123 (1):168-176.

32. Adib ZM, Ghanbarzadeh S, Kouhsoltani M, Khosroshahi AY, Hamishehkar H. The effect of particle size on the deposition of solid lipid nanoparticles in different skin layers: a histological study. Advanced Pharmaceutical Bulletin, 2016;6 (1):31.
33. Fresta M, Mancuso A, Cristiano MC, Urbanek K, Cilurzo F, Cosco D, Iannone M, Paolino D. Targeting of the pilosebaceous follicle by liquid crystal nanocarriers: In vitro and in vivo effects of the entrapped minoxidil. Pharmaceutics, 2020;12 (11):1127.
34. Li J-J, Li Z, Gu L-J, Choi K-J, Kim D-S, Kim H-K, Sung C-K. The promotion of hair regrowth by topical application of a Perilla frutescens extract through increased cell viability and antagonism of testosterone and dihydrotestosterone. Journal of natural medicines, 2018;72 (1):96-105.
35. Lee BH, Lee JS, Kim YC. Hair growth-promoting effects of lavender oil in C57BL/6 mice. Toxicological research, 2016;32:103-108.
36. Elsayed I, Abdelbary AA, Elshafeey AH. Nanosizing of a poorly soluble drug: technique optimization, factorial analysis, and pharmacokinetic study in healthy human volunteers. International Journal of Nanomedicine, 2014;9:2943.
37. Ravi PR, Aditya N, Kathuria H, Malekar S, Vats R. Lipid nanoparticles for oral delivery of raloxifene: optimization, stability, in vivo evaluation and uptake mechanism. European Journal of Pharmaceutics and Biopharmaceutics, 2014;87 (1):114-124.
38. Parhi R, Terapalli BR, Teja B. Formulation and in vitro evaluation of minoxidil topical gel. Turk J Pharm Sci, 2014;11 (2):153-162.
39. Xiao L, Zhang X, Chen Z, Li J, Li B, Li L. Molecular pathways involved in promoting activity of timosaponin BII on hair growth in C57BL/6 mice. BioMed Research International, 2020;2020.
40. Zhang Y, Wang J-w, Qu F-z, Zhang Y-m, Su G-y, Zhao Y-q. Hair growth promotion effect of cedrol cream and its dermatopharmacokinetics. RSC advances, 2018;8 (73):42170-42178.
41. Park S-O, Park B-S, Noh G-Y. Action mechanism of natural plant extracts for hair loss prevention and hair growth promotion in C57BL/6 mice. International Journal Of Pharmacology, 2015;11 (6):588-595.
42. Rajendran RL, Gangadaran P, Bak SS, Oh JM, Kalimuthu S, Lee HW, Baek SH, Zhu L, Sung YK, Jeong SY. Extracellular vesicles derived from MSCs activate dermal papilla cell in vitro and promotes hair follicle conversion from telogen to anagen in mice. Scientific reports, 2017;7 (1):1-12.
43. Kwon TR, Oh C, Park H, Han H, Ji H, Kim B. Potential synergistic effects of human placental extract and minoxidil on hair growth-promoting activity in C 57 BL/6 J mice. Clinical and Experimental Dermatology, 2015;40 (6):672-681.
44. Aldhalimi MA, Hadi NR, Ghafil FA. Promotive effect of topical ketoconazole, minoxidil, and minoxidil with tretinoin on hair growth in male mice. International Scholarly Research Notices, 2014;2014.
45. Choi N, Shin S, Song SU, Sung J-H. Minoxidil promotes hair growth through stimulation of growth factor release from adipose-derived stem cells. International Journal of Molecular Sciences, 2018;19 (3):691.
46. Berger R, Fu J, Smiles K, Turner C, Schnell B, Werchowski K, Lammers K. The effects of minoxidil, 1% pyrithione zinc and a combination of both on hair density: a randomized controlled trial. British Journal of Dermatology, 2003;149 (2):354-362.
47. Tricarico D, Maqoud F, Curci A, Camerino G, Zizzo N, Denora N, Cutrignelli A, Laquintana V, Lopalco A, la Forgia F. Characterization of minoxidil/hydroxypropyl-β-cyclodextrin inclusion complex in aqueous alginate gel useful for alopecia management: Efficacy evaluation in male rat. European Journal of Pharmaceutics and Biopharmaceutics, 2018;122:146-157.
48. Chandrashekar B, Nandhini T, Vasanth V, Sriram R, Navale S. Topical minoxidil fortified with finasteride: An account of maintenance of hair density after replacing oral finasteride. Indian dermatology online journal, 2015;6 (1):17.
49. Mahe YF, Cheniti A, Tacheau C, Antonelli R, Planard-Luong L, de Bernard S, Buffat L, Barbarat P, Kanoun-Copy L. Low-Level Light Therapy Downregulates Scalp Inflammatory Biomarkers in Men With Androgenetic Alopecia and Boosts Minoxidil 2% to Bring a Sustainable Hair Regrowth Activity. Lasers in Surgery and Medicine, 2021;53 (9):1208-1219.
50. Zappacosta AR. Reversal of baldness in patient receiving minoxidil for hypertension. The New England Journal of Medicine, 1980;303 (25):1480-1481.
51. Limas CJ, Freis ED. Minoxidil in severe hypertension with renal failure: effect of its addition to conventional antihypertensive drugs. The American journal of cardiology, 1973;31 (3):355-361.
52. Mehta PK, Mamdani B, Shansky RM, Mahurkar SD, Dunea G. Severe hypertension: Treatment with minoxidil. Jama, 1975;233 (3):249-252.
53. Boden WE, Korr KS, Bough EW. Nifedipine-lnduced Hypotension and Myocardial Ischemia in Refractory Angina Pectoris. Jama, 1985;253 (8):1131-1135.
54. Wester RC, Maibach HI, Guy RH, Novak E. Minoxidil stimulates cutaneous blood flow in human balding scalps: pharmacodynamics measured by laser Doppler velocimetry and photopulse plethysmography. Journal of Investigative Dermatology, 1984;82 (5):515-517.
55. Bunker C, Dowd PM. Alterations in scalp blood flow after the epicutaneous application of 3% minoxidil and 0.1% hexyl nicotinate in alopecia. British Journal of Dermatology, 1987;117 (5):668-669.
56. Fang C-L, Aljuffali IA, Li Y-C, Fang J-Y. Delivery and targeting of nanoparticles into hair follicles. Therapeutic delivery, 2014;5 (9):991-1006.
57. Matos BN, Reis TA, Gratieri T, Gelfuso GM. Chitosan nanoparticles for targeting and sustaining minoxidil sulphate delivery to hair follicles. International journal of biological macromolecules, 2015;75:225-229.
58. Li M, Marubayashi A, Nakaya Y, Fukui K, Arase S. Minoxidil-induced hair growth is mediated by adenosine in cultured dermal papilla cells: possible involvement of sulfonylurea receptor 2B as a target of minoxidil. Journal of Investigative Dermatology, 2001;117 (6).
59. Lopedota A, Denora N, Laquintana V, Cutrignelli A, Lopalco A, Tricarico D, Maqoud F, Curci A, Mastrodonato M, la Forgia F. Alginate-based hydrogel containing minoxidil/hydroxypropyl-β-cyclodextrin inclusion complex for topical alopecia treatment. Journal of Pharmaceutical Sciences, 2018;107 (4):1046-1054.
60. Mali N, Darandale S, Vavia P. Niosomes as a vesicular carrier for topical administration of minoxidil: formulation

CC BY

and in vitro assessment. Drug delivery and translational research, 2013;3 (6):587-592.
61. Mura S, Manconi M, Sinico C, Valenti D, Fadda AM. Penetration enhancer-containing vesicles (PEVs) as carriers for cutaneous delivery of minoxidil. International journal of pharmaceutics, 2009;380 (1-2):72-79.
62. Mura S, Manconi M, Valenti D, Sinico C, Vila AO, Fadda AM. Transcutol containing vesicles for topical delivery of minoxidil. Journal of drug targeting, 2011;19 (3):189-196.
63. Zhao Y, Brown MB, Jones SA. The effects of particle properties on nanoparticle drug retention and release in dynamic minoxidil foams. International journal of pharmaceutics, 2010;383 (1-2):277-284.
64. Uprit S, Sahu RK, Roy A, Pare A. Preparation and characterization of minoxidil loaded nanostructured lipid carrier gel for effective treatment of alopecia. Saudi Pharmaceutical Journal, 2013;21 (4):379-385.
65. Padois K, Cantiéni C, Bertholle V, Bardel C, Pirot F, Falson F. Solid lipid nanoparticles suspension versus commercial solutions for dermal delivery of minoxidil. International journal of pharmaceutics, 2011;416 (1):300-304.
66. Aljuffali IA, Sung CT, Shen F-M, Huang C-T, Fang J-Y. Squarticles as a lipid nanocarrier for delivering diphencyprone and minoxidil to hair follicles and human dermal papilla cells. The AAPS journal, 2014;16 (1):140-150.
67. Blume-Peytavi U, Massoudy L, Patzelt A, Lademann J, Dietz E, Rasulev U, Bartels NG. Follicular and percutaneous penetration pathways of topically applied minoxidil foam. European Journal of Pharmaceutics and Biopharmaceutics, 2010;76 (3):450-453.
68. Liao A-H, Lu Y-J, Lin Y-C, Chen H-K, Sytwu H-K, Wang C-H. Effectiveness of a layer-by-layer microbubbles-based delivery system for applying minoxidil to enhance hair growth. Theranostics, 2016;6 (6):817.
69. Lim SH, Kathuria H, Tan JJY, Kang L. 3D printed drug delivery and testing systems—a passing fad or the future? Advanced drug delivery reviews, 2018;132:139-168.
70. Kathuria H, Li H, Pan J, Lim SH, Kochhar JS, Wu C, Kang L. Large size microneedle patch to deliver lidocaine through skin. Pharmaceutical research, 2016;33 (11):2653-2667.
71. Kathuria H, Fong MH, Kang L. Fabrication of photomasks consisting microlenses for the production of polymeric microneedle array. Drug delivery and translational research, 2015;5 (4):438-450.
72. Kathuria H, Kochhar JS, Kang L. Micro and nanoneedles for drug delivery and biosensing. Vol 9: Future Science; 2018:489-492.

(cc) BY